MAUSAM, **76**, 4(October 2025), 1193-1206

MAUSAM

DOI: https://doi.org/10.54302/mausam.v76i4.7064
Homepage: https://mausamjournal.imd.gov.in/index.php/MAUSAM

UDC No.551.553.21:551.509.313

Assessing the dynamics and thermodynamics of monsoon onset: the impact of ENSO

SMRUTISHREE LENKA[1*], K. C. GOUDA[2#], MOHAN. T. S[1&], RANI DEVI[3] and V. S. PRASAD[1$]

[1]*National Centre for Medium-Range Weather Forecasting, Ministry of Earth Sciences, India*

(&drmohanthota@gmail.com, $vsprasad@ncmrwf.gov.in)

[2]*CSIR Fourth Paradigm Institute, Wind tunnel Road, Bangalore-37(*#drkrushnachandragouda@gmail.com,)

[3]*India Meteorological Department, Ministry of Earth Sciences, Lodi Road, New Delhi – 110 003, India*

(anijangra1992@gmail.com)

(*Received 22 April 2025, Accepted 21 August 2025*)

***Corresponding author's email: smruti.swati@gmail.com**

सार – यह अध्ययन प्रमुख गतिकीय और ऊष्मागतिकीय प्रक्रियाओं का विश्लेषण करके भारतीय उपमहाद्वीप में मानसून के आगमन और प्रगति में शामिल तंत्रों की जाँच करता है। इसके अतिरिक्त, यह विभिन्न ENSO चरणों के दौरान मानसून के आगमन की विशेषताओं की भी जाँच करता है। इसके लिए, हमने मानसून के आगमन और संबंधित विशेषताओं पर एक व्यापक अध्ययन करने के लिए दीर्घकालिक अवलोकनों और ERA5 पुनर्विश्लेषण डेटा का उपयोग किया।

परिणाम दर्शाते हैं कि, सक्रिय मानसून शियर डोमेन (MSD) और केरल डोमेन (KD) दोनों में क्षेत्रीय और देशांतर दोनों दिशाओं में तापीय प्रवणता और संबंधित ऊर्ध्वाधर पवन कतरनी के बीच एक मजबूत संबंध है। यह पाया गया है कि, यह संबंध विभिन्न समय पैमानों यानी वार्षिक, मौसमी (ISM-लंबाई) और शुरुआत पंचम (p0) पर भिन्न होता है, जो रेखांकित करता है कि मानसून संवहन की तीव्रता तापीय प्रवणता और पवन कतरनी पर निर्भर करती है। विश्लेषण से यह निष्कर्ष निकलता है कि कमजोर ऊर्ध्वाधर पवन कतरनी की उपस्थिति एक स्थिर स्थिति बनाती है और एक महत्वपूर्ण तापीय प्रवणता की उपस्थिति, जो विभिन्न ऊंचाइयों पर हवा की गति और दिशा में न्यूनतम बदलावों की विशेषता है, महत्वपूर्ण कारक हैं जो मानसून की शुरुआत को सुविधाजनक बनाते हैं। इसके अलावा, अल नीनो भारतीय उपमहाद्वीप पर पवन कतरनी को बढ़ाता है और मानसून की शुरुआत में देरी करता है तापमान प्रवृत्ति समीकरण का विश्लेषण एक प्रबल डायबेटिक तापन प्रदर्शित करता है जो गिल-जैसी रॉस्बी तरंग प्रतिक्रिया से जुड़ा है, जो मध्य-अक्षांशीय पश्चिमी जेट के साथ ऊष्मागतिकीय अंतःक्रियाओं की शुरुआत करता है। इसके अलावा, यह अध्ययन मध्य प्रशांत (सीपी) के गर्म होने की घटनाओं और मानसून की शुरुआत की विशेषताओं पर इसके प्रभाव का भी संकेत देता है, जिस पर और अधिक शोध की आवश्यकता है।

ABSTRACT. This study examines the mechanisms involved in the onset and progression of the monsoon over the Indian subcontinent by analyzing key dynamical and thermodynamical processes. Additionally, it investigates the characteristics of monsoon onset during various ENSO phases. To achieve this, we utilized long-term observations and ERA5 reanalysis data to conduct a comprehensive study on the onset and related characteristics.

Results indicate that, a robust connection between the thermal gradient in both zonal and meridional directions and the corresponding vertical wind shear both across the active monsoon shear domain (MSD) and Kerala domain (KD). It is found that, this relationship varies across different time scales i.e., annual, seasonal (ISM-length), and onset pentad (p0), underscoring that the intensity of monsoon convection hinges on the thermal gradient and wind shear. The analysis concludes that presence of weak vertical wind shear, creates a stable state and the presence of a significant thermal gradient, characterized by minimal variations in wind speed and direction at different altitudes, are critical factors that facilitate the monsoon onset. Further, El Niño tends to increase wind shear over the Indian subcontinent and leads to a delayed monsoon onset. Elevated geopotential height during an El Niño year indicates the existence of a high-pressure region, which is an unfavorable condition for the onset of the monsoon. Analysis of temperature tendency equation exhibit a robust diabatic heating which is linked to a Gill-like Rossby wave response, initiating thermodynamic interactions with midlatitude

westerly jet. Furthermore, this study also gives an indication of the influence of central pacific (CP) warming events and its influence on monsoon onset characteristics, which needs further exploration.

Key words – Monsoon onset, Thermal gradient, ENSO, Apparent heat source, Moisture sink, wind-shear.

1. Introduction

India receives the most significant portion of its annual rainfall during the principal rainy season *i.e*. June-September (Gadgil *et al.*, 2003; Jain *et al*., 2012). The commencement of the rainy season (or the monsoon "onset") over the Indian subcontinent during boreal summer plays a major role in dictating the season rainfall amounts. The onset of the Indian summer monsoon (ISM) is a highly anticipated meteorological phenomenon as it provides the signature of the rainfall transition from summer to the monsoon season and significantly affects the agricultural productivity of the country (Webster *et al*., 1998; Gadgil, 2003; Moron & Robertson, 2014). The onset of the ISM is characterized by a fast transition from a dry and warm season, with the easterly flow at lower levels and westerly flow at upper levels, to a wet season, with lower-level westerlies and upper-level easterlies (Geen *et al*., 2020). The convection linked to the ISM represents the most substantial contributor to atmospheric heating due to upper-level divergent circulation (Hoskins & Rodwell, 1995; Yanai & Tomita, 1998). Further, the onset of ISM has a very strong association with one of the dominant tropical oscillations called El Niño Sothern Oscillation (ENSO) (Ashok *et al*., 2004). Despite, its societal impacts, the dynamics and thermodynamics associated with the monsoon onset are still poorly understood. In this research work, both dynamics and thermodynamical perspectives of the monsoon onset and how it is influenced by the ENSO modes, especially during the El Niño is examined.

In general, the southwest monsoon onset over India is usually marked by the arrival of copious amounts of rainfall in the state of Kerala, located in the southwestern part of India (Soman & Kumar, 1993). Kerala often experiences the first monsoon showers, marking the official onset date, which is typically around 1st June. After the onset of ISM, it gradually progresses poleward by the influence of favorable meteorological conditions (shear, specific humidity etc.) and covers the entire Indian subcontinent over the next few weeks to months (Ananthakrishnan & Soman, 1988) and the onset timing and occurrence of this progression exhibits a strong interannual variability (Lenka *et al*., 2024). Note that, due to the heterogeneity in onset dates over the Indian subcontinent, recently, the India Meteorological Department (IMD) has observed the onset over Northwestern parts of India is slightly earlier, 8th July, compared to the previous date of 15th July. The onset of ISM is characterized by significant changes in convection and circulation over the Indian subcontinent and its surrounding regions (Rao, 1976; Hastenrath & Greischar, L.1991; Fasullo & Webster, 2003; Kripalani *et al*, 2003; Wang *et al*., 2009; Gadgil, 2018). The main source of convection over the Indian subcontinent is due to the presence of two oceanic maxima, located in the Arabian Sea (AS) and the Bay of Bengal (BOB), respectively. The monsoon circulation over the South Asia in zeroth order is essentially an atmospheric response to the temperature contrast between land and ocean induced by the movement and heating of the sun, leading to significant variability (Wang & Ding, 2008). Some studies confirmed that intense solar heating and associated thermodynamical conditions produce sufficient convection resulting in the poleward shifting of the Intertropical Convergence Zone (ITCZ) (Privé & Plumb 2007; Gadgil, 2018), which plays a significant role in influencing the wind shear and circulation patterns and, consequently, the onset of the ISM (Lenka *et al*., 2024).

To comprehend the dynamics of the monsoon onset, it is essential to grasp the significance of various factors, (such as thermal gradient, vertical wind shear *etc.*) that play a pivotal role in molding weather patterns (Li and Yanai, 1996, Duan *et al*., 2008). Earlier, studies have shown the impacts of thermal gradients (Weldeab *et al*., 2022) and wind shear in shaping the timing of the monsoon onset. In addition, Strong vertical wind shear can hinder the development of the monsoon by disrupting convergence and low-level jet formation and its variability is essential for initiating and maintaining the monsoon circulation (Wilson & Mohanakumar, 2020). Numerous studies, used indices, based on wind shear to precisely quantify and analyze the dynamics of the monsoon. For example, the Webster Yang Index (WYI), reflects the intensity of both the low-level westerly jet and the upper-level easterly jet. (Webster & Yang, 1992). Later, Goswami *et al*., (1999) studied the Monsoon Hadley Circulation Index MCI, computed wind shear using the winds at two levels (850 and 200 hPa) and averaged over a broader region extending further north (10°-30° N) and east (70°-110° E). In another study, Douglas (1992) identified the average easterly wind shear, was a crucial parameter for the northward advancement of the monsoon convection band. A modified version of the MCI, namely the Shinu-Mohan index (SMI), excluding the topographical influences on the zonal wind pattern is utilized (Wilson & Mohanakumar, 2020). The importance of shear and its strong coherence with rainfall over the monsoon shear domain (MSD) is elaborately studied by Gouda and Goswami (2016). Numerous other studies have also highlighted the significance of the vertical wind shear in the context of the ISM (Parthasarathy and Yang., 1995; Prasad and Hayashi,

2005; Sahana *et al*., 2015; Gouda & Goswami, 2016; Athira *et al*., 2023). Thus, understanding wind shear and its interaction with key meteorological variables and dynamical processes is essential for predicting the timing and behaviour of the monsoon onset and progress, this forms one of the scientific issues of the present study.

Another crucial aspect which dictates the monsoon onset is the ENSO and Indian Ocean Dipole (IOD) teleconnections. Observational evidence of the ENSO-monsoon rainfall connection reveals that the enduring association between the Indian and tropical pacific region SST (Ashok *et al*., 2004; Roy *et al*., 2016; Lenka *et al*., 2022;). The abnormal rise in pre-monsoon temperatures disrupts the land-ocean thermal gradient (Devi *et al*., 2022, 2023), potentially contributing to the development of large-scale climate phenomena *e.g*., ENSO, IOD. This disruption can thereby influence the ISM onset and rainfall distribution (Ashok *et al*., 2003; Yamada *et al*., 2022).

From the earlier studies, it is evident that wind shear and thermal gradients are essential in studying monsoons, as they significantly influence the development, strength, and variability of these systems (Webstar *et al*., 1998). By analyzing the combined effect of the wind shear, and thermal gradients during the ENSO phases over the Indian subcontinent during the monsoon onset, will shed light on 1) the atmospheric dynamics and the thermodynamical aspects which help in understanding and quantifying the contribution of the physical drivers of monsoon and its onset, 2) the dynamical impact of the large-scale process *i.e*. ENSO phenomenon on vertical wind shear and thermal gradient over the study region, which in turn affect the monsoon onset and its circulation both in space and time. This examination aims to contribute to a better scientific understanding of the complex dynamical impact of various atmospheric parameters on ISM onset. This insight is significant as the accurate and timely forecasting of monsoon patterns can exert substantial influence on planning, productivity, and overall socio-economic stability. The paper is structured as follows, in Section 2, an overview of the data sets used in this research and methodology employed for computing vertical wind shear, thermal gradient, ISM-length along with the TDE are presented. The results are discussed in the section 3 followed by summary and conclusion in section 4.

2. Data and methodology

2.1. *Reanalysis data*

In the present work, we have used the 5th generation European Center for Medium-Range Weather Forecast Reanalysis (ERA5) with a spatial resolution of 0.25° (approximately 28 km), having 27 pressure levels between 100 and 1000 hPa for the study period 1981-2020 (40) years is utilized (Hersbach *et al*., 2020). ERA5 estimated daily zonal and meridional (u, v) winds along with Temperature (T) and vertical p-velocity (w) is also utilizes. In addition, we have also used the monthly surface 2 m temperature.

2.2. *Rainfall observations and ISM characteristics*

In the present study the rainy season length, referred as ISM-length is used following the procedure by Lenka *et al*., 2024. The duration of the monsoon season is calculated for each year instead of confining the fixed June-September (*i.e*., JJAS, 122 days). The duration between the onset and withdrawal date of ISM is defined as the rainy season length (ISM-length) and ISM onset and withdrawal are calculated using cumulative rainfall anomaly technique (Lenka *et al*., 2024). For the computation of ISM length, India Meteorological Department (IMD) 0.25 deg gridded daily data also used for the period from 1951-2020. For more details about the IMD rainfall data please refer to Pai *et al.,* 2014. *i.e.*

$$ISM\text{-}length\ (i, j, day, year) = WD\ (i, j, year) - OD\ (i, j, year) \quad (1)$$

where, WD represents the withdrawal date, and OD represents the onset date at the grid point (i, j) in any given monsoon season. A pentad analysis (p0) of the composite average of various meteorological parameters over 40 years are computed. The onset pentad (p0), includes the onset date along with the 2 preceding and 2 following days. The domain averaged wind shear and thermal gradient over the said two domains are considered for the present analysis. The pentad (p0) analysis has been conducted to assess the influence of the ENSO on wind shear, thermal gradient, geopotential height and the onset of the ISM. In addition, we defined the onset categories (*e.g* late and early) based on one standard deviation (σ) from the climatological mean onset date (IMD declared onset dates). Years with onset dates greater than $+1\sigma$ were classified as late onset, while those earlier (than -1σ) were classified as early onset. The normal onset years fall within $\pm 1\ \sigma$ of the mean onset date.

2.3. *Methodology*

In this section, a detailed description of the parameters used to study the onset characteristics are given, they include 1) Thermal gradient, 2) vertical wind shear, and 3) the thermodynamic energy equation is given.

(*i*) *Thermal gradient*

In the current study, the central difference method is employed to compute the thermal gradient of the temperature at a given point *x*, is computed as

$$\frac{d}{dx} = \frac{T(x+\Delta x)-T(x-\Delta x)}{2\Delta x} \quad (2)$$

Here, T(x) represents temperature at point *x*, and Δx is the grid spacing between neighboring data points. Both the zonal and meridional thermal gradient is computed using the above-mentioned method.

Meridional Thermal Gradient (MTG): MTG gives the rate of temperature change per unit of latitude

$$MTG(i,j,t) = \frac{1}{P}\sum_{i=1}^{P}\frac{dT(i)}{dx} \quad (3)$$

Zonal Thermal Gradient (ZTG): The ZTG gives the rate of temperature change per unit of longitude

$$\text{ZTG} = \frac{1}{Q}\sum_{j=1}^{Q}\frac{dT(j)}{dy} \quad (4)$$

where, *dT(i) =T(i,j)-T(i+1,j)* and *dT(j)=T(i,j)-T(i,j+1)*

The zonal and meridional averaged thermal gradient is obtained using the following equations

$$MTG(t) = \frac{1}{PQ}\sum_{j=1}^{Q}\sum_{i=1}^{P}MTG(i,j,t) \quad (5)$$

$$ZTG(t) = \frac{1}{PQ}\sum_{j=1}^{Q}\sum_{i=1}^{P}ZTG(i,j,t) \quad (6)$$

(*ii*) *Vertical Wind Shear*

The vertical shear of horizontal wind is computed by taking difference between the upper reference vertical level is fixed at 200 hPa, while the examination encompasses the 850 hPa and 1000 hPa levels as potential lower reference level.

Vertical wind shear at lower pressure level ***l*** (1000 hPa or 850 hPa) with respect to the upper vertical pressure level ***u*** *(*200hPa) for each day of a particular year at each grid point *(i, j)* is computed as

$$Ws(i,j,t) = \sqrt{\left(U_l(i,j,t) - U_u(i,j,t)\right)^2 + \left(V_l(i,j,t) - V_u(i,j,t)\right)^2} \quad (7)$$

where $U_l(i,j,t)$ represent the low level (1000/850 hPa) zonal wind at latitude *i*, longitude *j* and time *t* and $U_u(i,j,t)$ represent the upper level (200 hPa) U wind at latitude *i*, longitude *j* and time *t.* Similarly, the same notation used for the meridional wind *i.e.* $V_l(i,j,t)$ and $V_u(i,j,t)$.

Two distinct domains i.e. monsoon core and onset region, have been selected for the analysis of wind shear and thermal gradient. MSD extending in the region of 65°-100° E longitudes and 5°-40° N latitude following the earlier study (Gouda & Goswami, 2016) KD representing the monsoon onset zone extending in longitudes 74.5°-77.5° E and latitudes 8°-13° N.

The daily domain averaged vertical wind shear $WsD(t)$ computed at two vertical levels for the day 't' is calculated as follows

$$WsD(t) = \frac{1}{XY}\sum_{j=1}^{Y}\sum_{i=1}^{X}Ws(i,j,t) \quad (8)$$

where X and Y corresponds to the count of number of grid points in the meridional and zonal direction in the respective domains

(*iii*) *Heat and moisture equations*

In the present work, the dry static energy that represents the total energy content of a unit mass of dry air in the atmosphere is used for analyzing and understanding atmospheric stability, vertical motion, and other thermodynamic aspects of the atmosphere. By employing the mass continuity, heat energy, and moisture continuity equations, the atmospheric energy and moisture budget equations can be derived (Yanai *et al*., 1973). The atmospheric apparent heat source (Q1) can be calculated as following.

$$Q1 = q1 \cdot Cp = Cp\frac{\partial T_m}{\partial t} - Cp(\omega\sigma - V\cdot\nabla T_m) \quad (9)$$

where, Q1 represent the net heat source and net moisture sink. Cp = specific heat at constant pressure (Cp=1004.64 $J(Kkg)^{-1}$); Tm = Mean air temperature; ω = Vertical wind velocity; σ = Static stability; V (u, v) = Horizontal wind velocity.

The vertically integrated forms of Q1 can be expressed as $\langle Q1\rangle$

$$\langle Q1\rangle = \frac{1}{g}\int_{250hPa}^{700hPa}(Q1)dp \quad (10)$$

The initial term on the right-hand side of Equation 9 signifies the local temperature tendency. 2nd term

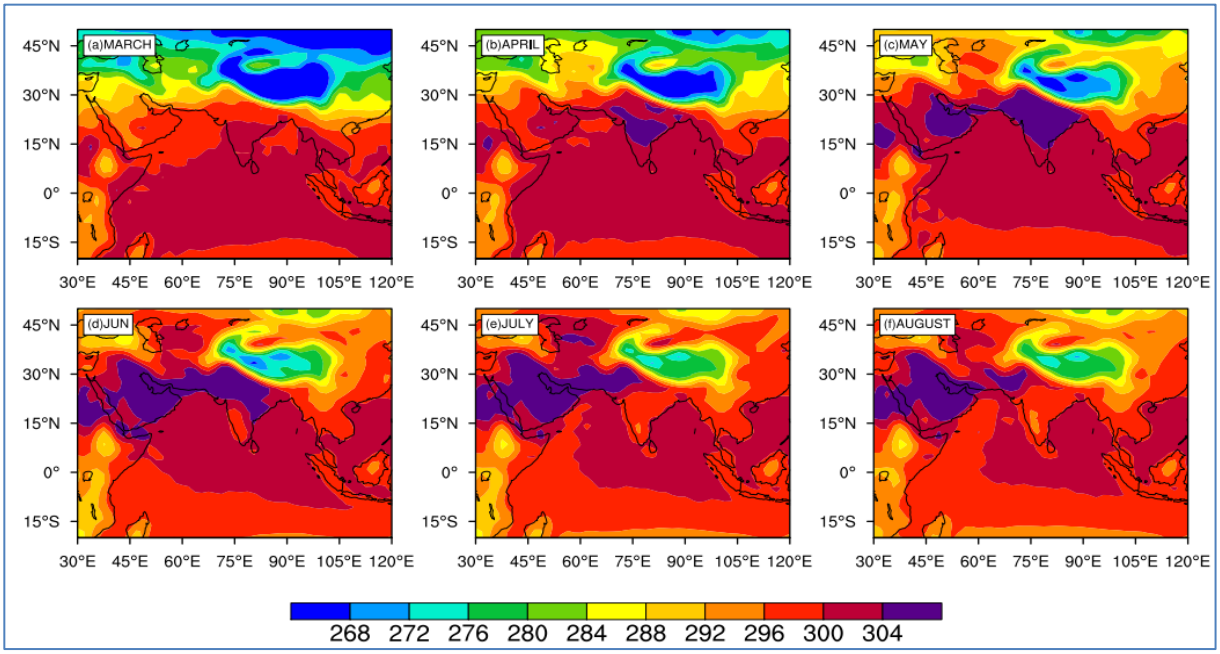

Figs. 1(a-f). Climatological (1951-2022) 2-meter surface temperature (K) during March, April, May, June, July and August from NCEP reanalysis-I

represents the static stability whereas the last term corresponds to the horizontal advection. The residual term of Eq. (9) *i.e*. Q1 has been noted as diabetic heating term. Diabetic heating increases due to four components, namely outgoing long wave radiation (OLR), incoming shortwave radiation, latent heating, and turbulent mixing of air.

(*iv*) *Composite analysis*

In the manuscript, some of the figures are prepared using the composite technique, and it is briefly given below: Composite spatial and temporal maps were prepared by averaging the anomalies of selected variables over the categorized years (*e.g* El-Nino and La-Nina), with spatial averaging carried out over the specified domain.

3. Result and discussion

3.1. *Mean state*

(i) Differential heating

In this section, the climatological (1981-2020) evaluation of the 2-m temperature during March - August (regarded as the pre-monsoon, pre-onset and monsoon periods) has been examined and it is presented in Fig. 1. The monthly spatial distribution illustrates a consistent increase in temperatures over the Indian subcontinent and the Tibetan Plateau (TP) region from March to August. A noticeable seasonal transition from the pre-monsoon period to the monsoon period is observed, indicating an increase in temperature not only over the TP but also over the Indian landmass. The surface temperature over the Indian Ocean consistently remains warm during March-July, exhibiting large spatio-temporal variations. Further, the analysis of the land-ocean thermal gradient shows a notable gradient during the months of May and June (ISM onset months, Figure not shown). During summer, the land undergoes more rapid heating compared to the adjacent ocean attributing to the land's smaller specific heat and shallower depth. Varied heat capacities of land and water result in differential heating, with land heating up more quickly than the ocean. As there is approximately a fourfold difference in the specific heat between the dry land and water (Abu-Hamdeh, 2003).

The monthly tendency (Figure not shown) also illustrates a consistent increase in the intensity of land surface warming during the pre-monsoon period. The land surface of the Indian subcontinent exhibits higher temperatures in April and May compared to March and April, respectively. Gradually, the land surface temperature begins to decrease in June. This decrease in land temperature transitions from Southern India to the central part of India, resulting in a decline in surface temperature over this region from June to July. A comparable pattern of tendency is also observed in the Tropical Indian Ocean. The ocean surface temperature experiences an increase in

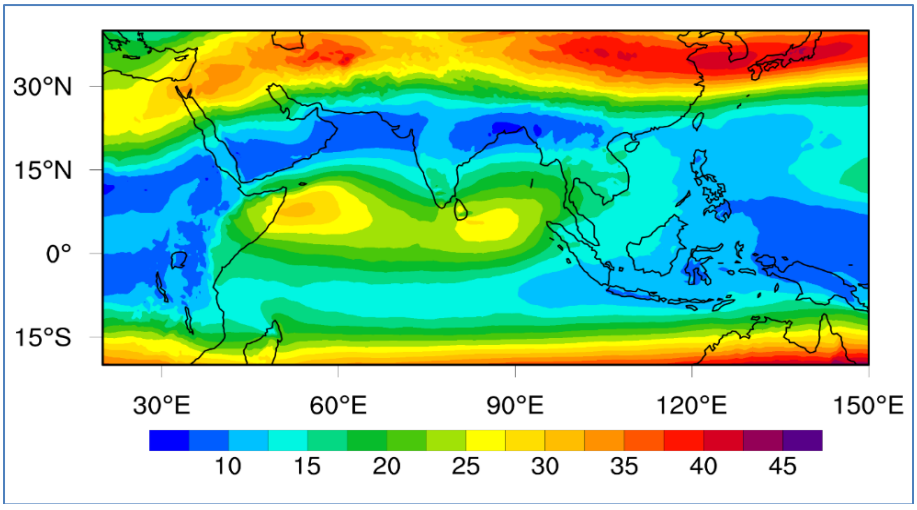

Fig. 2. Spatial distribution of wind shear climatology (1951-2022) at (a) 850hPa. The map is prepared by, averaging the wind shear data during onset pentad (see details in section 2)

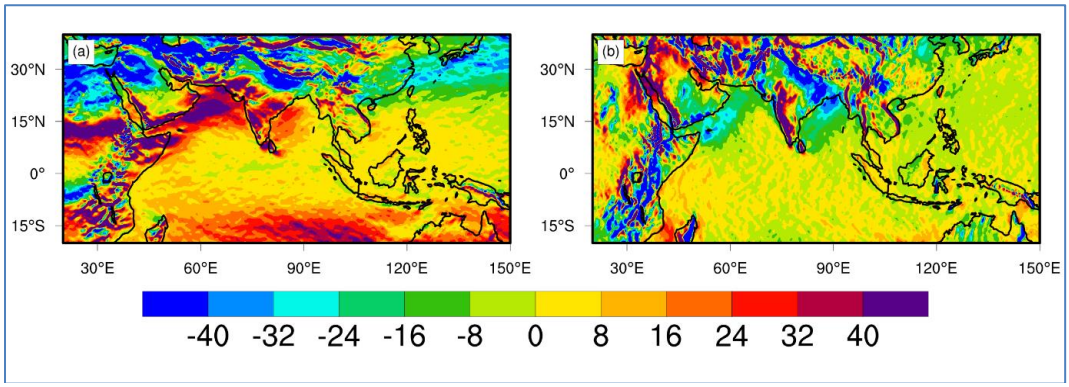

Figs. 3(a&b). Spatial distribution of (a) zonal and (b) meridional thermal gradient climatology (1951-2022). The map is prepared by, averaging the thermal gradients during onset pentad (see details in section 2)

warming intensity in April and May compared to March and April, respectively. Conversely, there is a decrease in temperature during June and July compared to May and June, respectively. The plots suggest that the warming intensity and temperature change are more pronounced over land than in the ocean. A distinct temperature shift occurs from the pre-monsoon phase to the onset and progress of ISM phases.

(ii) Wind shear

The wind shear conditions can vary from one monsoon region to another (*e.g.*, Indian Summer Monsoon, West African Monsoon, East Asian Monsoon) and exhibits a pronounced interannual variability. Low-level jet streams, characterized by their concentrated and robust wind patterns at lower altitudes, have the potential to impede the initiation of monsoons by obstructing moist air progression. Frequently, during the onset phase, there is a tendency for these jet streams to weaken or shift position (Belmecheri *et al*., 2017). Fig. 2 represents the lower tropospheric pentad vertical wind shear averaged at 850 hPa. A clear decrease in vertical wind shear is visible, which is generally favorable for the onset of ISM. Wind shear can lead to the formation of shear lines, which are boundaries where winds of different directions and speeds converge. These shear lines can act as focal points for the initiation of convection and rainfall (Webster *et al*., 1998), creating a conducive environment for the onset of ISM.

(*iii*) *Thermal gradient*

Another important aspect is the thermal gradient, the zonal and meridional gradients (ZTG and MTG) play crucial roles in the dynamics of the onset of ISM. For instance, the strong ZTG influences the establishment of the monsoon trough, a quasi-permanent low-pressure system responsible for drawing moist air from the Indian Ocean towards the Indian subcontinent (Fig. 3(a)). Thus, a

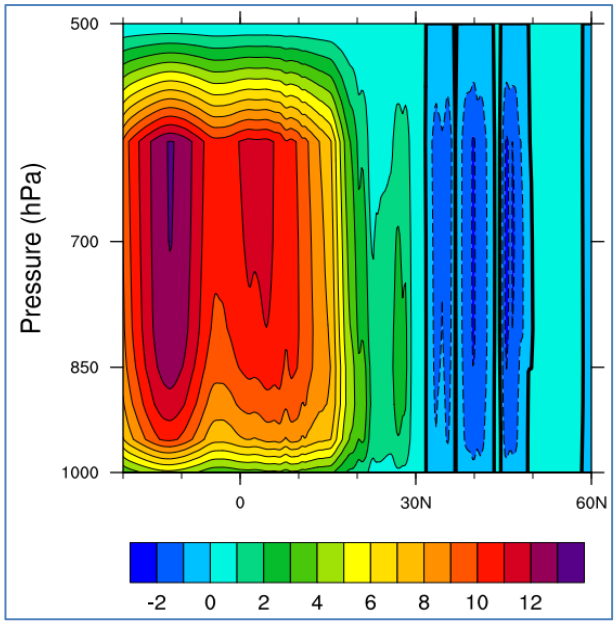

Fig. 4. Latitude-height profile depicting the mean meridional stream function (kg/s) for the onset pentad. Positive (negative) values signify the ascending (descending) branch of the Hadley circulation. The profile is computed by averaging the data between longitudes 60°-100° E

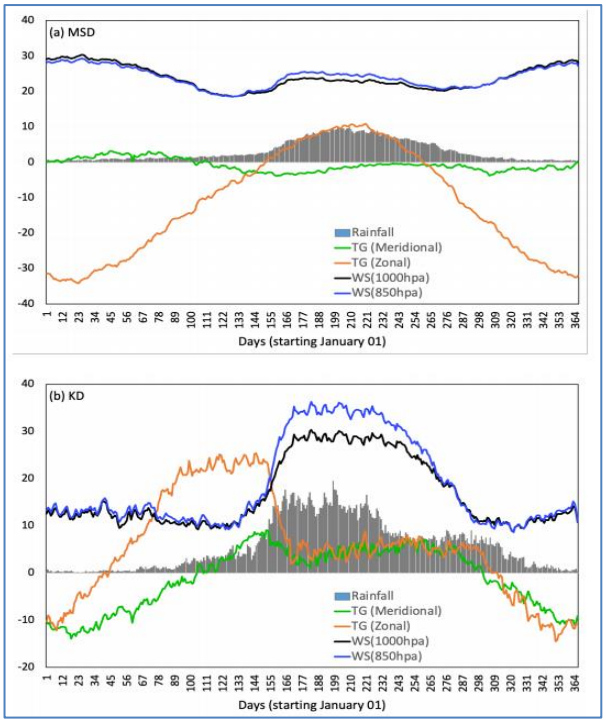

Figs. 5(a&b). The daily variation of zonal and meridional temperature gradient and vertical wind shear at 1000hPa and 850hPa (computed with respect to 200hPa) over the MSD domain (a) the Kerala domain (b). The period of analysis is 1951-2022. Different colors in the legend indicates temporal evolution of different variables

strong zonal gradient can help in creating the necessary conditions for the monsoon trough to form. The MTG can lead to the formation of Hadley cells, which are important components of the Earth's general circulation. Also, this gradient contributes to the movement of the ITCZ, which is closely associated with the monsoon onset (Fig.3(b)). This affirms the influence of wind shear in modulating the ITCZ, which further impact the timing and onset of monsoon rainfall, which will be discussed briefly in the following section.

(*iv*) *ITCZ*

To get insight into the ITCZ and ISM onset, the pentad mean meridional stream function presented in Fig.4. Although, a comprehensive understanding of the dynamics of evolving ITCZ regime to monsoon regime is out of the scope of the present work, for completeness, here we briefly describe the ITCZ and monsoon onset characteristics emphasizing the meridional stream function. In general, the location of ITCZ is determined by the presence of stream function, which reaches zero over a particular region. The positive and negative values of the mean meridional stream function, denoting the ascending and descending branches of the Hadley circulation respectively, offering a visual representation of the latitudinal extent of the ITCZ relative to the pressure level. From Fig.6 it is seen that the width of the ITCZ a key determinant of monsoonal rainfall intensity in tropical regions, is positioned around 30° N during this period over the Indian landmass. This observation strongly suggests that the presence of the ITCZ, is positioned around 30° N plays a crucial role in initiating and advancing the monsoon across India.

3.2. *Onset variability*

(i) Role of wind shear and thermal gradient

The daily averaged vertical shear of horizontal wind, both in the zonal and meridional directions, at 1000 hPa and 850 hPa levels, relative to the 200 hPa level, is presented for both domains MSD and KD (Fig.5). Along with the shear, the annual cycle of the zonal and meridional component of thermal gradient averaged across both the domain is also presented. This indicates a robust divergence in the annual cycles in the two domains, with a distinct and clear depiction of the changing seasons observed specifically within the MSD domain (Fig.5(a)) in comparison to the KD region (Fig.5(b)). For both the domains, the shear value is minimal during the pre-monsoon season, while it significantly decreases during the onset period. After the onset, the value rises considerably during the rainy season. Subsequently, the value gradually decreases indicating the withdrawal phase of ISM. The MTG conforms to a Gaussian distribution,

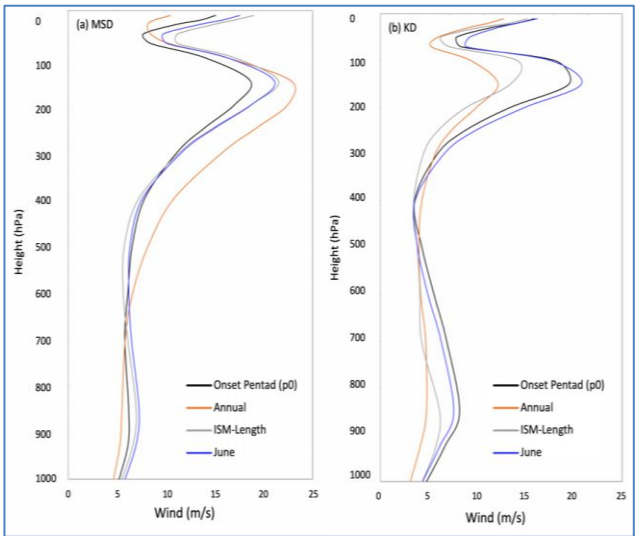

Figs. 6(a&b). Climatological (1951-2022) vertical wind profile averaged across various time scales i.e. annual, seasonal (ISM-length) and onset Pentad (p0) analyzed over (a) MSD and (b) KD

while the ZTG exhibits a nearly linear pattern in MSD domain. This suggests that the horizontal thermal gradient's variability is more pronounced in the latitudinal direction compared to the longitudinal distribution. However, in the KD domain, both the MTG and ZTG exhibit a similar pattern (Fig.5(b)).

The daily area averaged ISM rainfall, over the complete period has a strong coherence with the vertical wind shear and thermal gradient, averaged over the extensive spatial regions. The correlation analysis of thermal gradient and wind shear across MSD is provided in Table1, encompassing annual and seasonal (ISM-length) scales. The correlation analysis during the onset of ISM over KD as well as MSD also computed for p0. It's evident that at the annual scale, there is a robust positive correlation between the ZTG and wind shears, while a notably strong negative correlation is observed between the MTG and wind shear. However, during the monsoon season, this relationship is reversed, with a positive correlation emerging between the MTG and wind shear, leading to increased convection. The analysis over MSD and KD indicates a negative (positive) relation between zonal (meridional) thermal gradient & wind shear at both the vertical levels.

The climatological (1981-2020) vertical wind profiles, spatially averaged over the MSD and KD across various time scales is presented in Fig.6. The vertical structure of daily wind, averaged over annual, seasonal (ISM-length), monthly (June) and during the onset pentad (P0), highlights the distinct characteristics of daily vertical shear as the wind at 200 hPa reaches the maximum value of about 20 m/s. June is regarded as the initial month of the monsoon season, as the climatological onset of the monsoon is defined as the 1st of June. It is also observed that, in June the surface wind remains high compared to other time scales considered and the same analysis during onset pentad indicates that the value is higher above the 600 hPa. Similarly, during the onset, to know the vertical circulation pattern the analysis over KD indicates that the p0 time averaged wind is much stronger along with the June value, whereas the strength is lower in the annual and seasonal scale. This indicates the higher wind intensity resulted in wind shears below the low-level jet core and the onset prevails in KD region. So, the impact of wind shear and thermal gradient is more prominent during the onset phase compared to the annual and ISM-length time scales and so the KD region is considered for onset analysis.

(*ii*) *Thermodynamic aspects during ISM onset*

To obtain a more profound understanding of the predominant physical processes during monsoon onset, each parameter of the TDE has been examined thoroughly. The combined effects of both horizontal & vertical advection of air parcels, in addition to the impact of radiation flux in the air column between 700 hPa to 250 hPa is depicted (Fig.7). The horizontal advection in the TDE, represented by Eq. 9 indicates cold air from both the western & eastern regions of Indian landmass, is propelled by the horizontal advection of air parcels carried by the westerly winds at lower tropospheric levels (Fig.7(a)).

The values are notably stronger over the Indian landmass region and this robust advection drives the flow of moisture-laden air masses (Figure not shown) from the ocean towards the landmass, playing a pivotal role in shaping the moisture content and precipitation patterns, particularly during the onset of the monsoon. The combination of vertical advection and adiabatic warming is identified as the static stability (term 2 in Eq .9). The static stability remains constant, resulting the variations in the vertical velocity (Fig.7(c)) which is mainly balanced by the temperature advection (Fig.7(b)) and diabatic heating (Fig.7(d)). It is also demonstrated that, in the tropical regions the balance among the TDE terms are primarily dominated by diabatic heating, while the horizontal advection mainly influences the balances in extratropical or temperate regions, where horizontal gradients play a major role (Mohanty *et al*., 1983; Hoskins & Karoly, 1981). The upward motion observed in Indian Ocean, AS and BoB (Fig.7(c)) appears to be in corroboration with the diabatic heating (Fig.7(d)) occurring in those regions. The vertical advection of daily mean temperature (Fig.7(c)) exhibits a notably negative value over the AS and southwest coast of Indian region, signifying the robust convergence of air parcels. Simultaneously, a relatively low negative values of static stability parameter in TDE signify the omnipresence

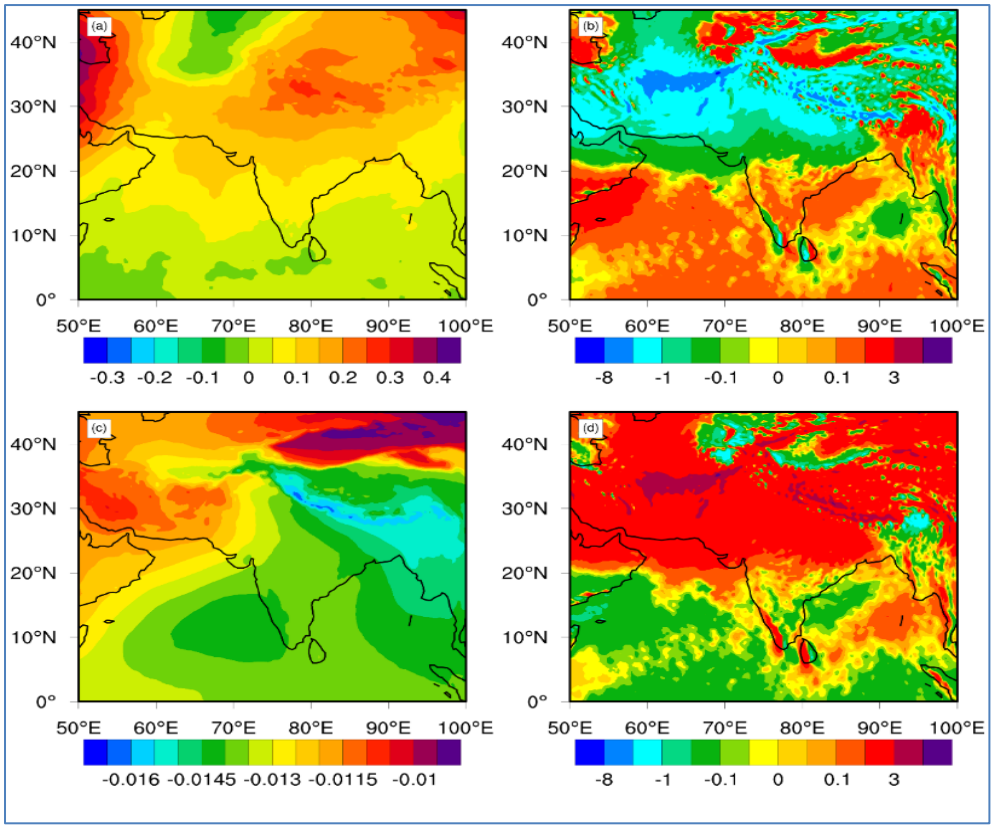

Figs. 7(a-d). Illustration of the four individual terms of the dry thermo-dynamic equation (TDE) at 500 hPa, namely (a) temperature advection (b) horizontal advection (c) static stability and (d) diabatic heating

TABLE 1

Correlation analysis of thermal gradient and wind shear across MSD for the period of 1981-2020. The correlation values presented in the Table are 90% significant.

Time scale	dt/dx vs 1000 hPa shear	dt/dy vs 1000 hPa shear	dt/dx vs 850 hPa shear	dt/dy vs 850 hPa shear
Annual-MSD	0.56	-0.85	0.53	-0.72
Seasonal (ISM-length)-MSD	-0.14	0.90	-0.21	0.91
Onset Pentad-MSD	-0.31	0.12	-0.27	0.14
Onset Pentad-KD	-0.51	0.25	-0.21	0.20

of instability (Fig.7(c)). These competing dynamical conditions contributes to the overall monsoon circulation over the Indian region. The elevated vertical advection values over northern India is also correlated with diabatic heating (Fig. 7(d)).

3.3. *ENSO impact on onset*

(*i*) *SST*

In the above sections, a comprehensive discussion of monsoon onset and its characteristics by utilizing the various dynamical (shear) and thermodynamical (TDE) is presented. Now, for better understanding the impacts of ENSO on ISM onset is present here, as ENSO modes serves as a large-scale predictor for extended range and seasonal prediction of monsoon and associated rainfall over south Asia regions through teleconnections. Thus, we anticipate that the results obtained from the current analysis will enhance our understanding of the ENSO-monsoon relationship. It is widely recognized that the warming of sea surface temperatures (SSTs) in the equatorial Pacific is a significant factor influencing the progression and development of the monsoon over the Indian subcontinent. However, in recent decades studies have identified that the warming is not only confined to eastern pacific regions but also spread towards central pacific (CP) regions too. Recent studies also reported that

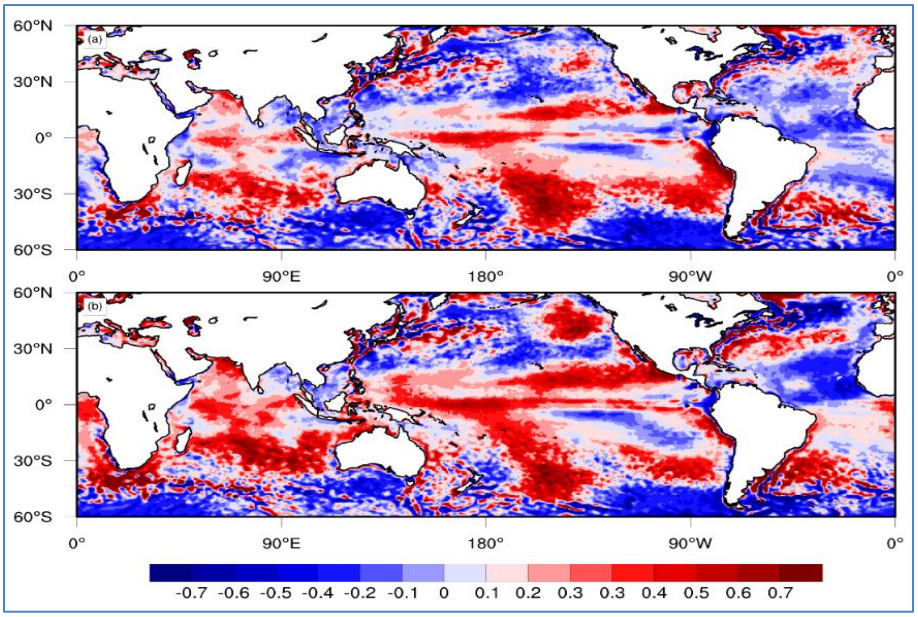

Figs. 8(a&b). Composite sea surface temperature (SST) anomalies for a) ElNino and b) central pacific (CP) ElNino year for March-April-May (MAM) months

the effect of CP warming is more over Indian ocean, which in-turn impacts the monsoon progression. Therefore, in the present work, along with the CP El Nino events and La Niña events, the influence of CP warming events on monsoon onset is also discussed.

Fig. 8 exhibits the spatial composite of SST anomaly pattern considering the March-April-May anomalies together during El Niño and CP warming years. From Fig.8(a) it is apparent that the eastern pacific warming especially along the south American coast is relatively weaker, during the MAM composite. In contrast the spatial anomalies are stronger and more spread towards central pacific regions during the CP events or years. It is interesting to see the SST anomalies over the Indian ocean is also large during the CP events compared to El Niño events. Similar spatial patterns are also seen during the DJF composite maps (Figure not shown), with an enhanced SST magnitude. This affirms the influence of SST anomalies over Indian ocean during the El Niño and CP warming periods. The ISM onset and its associated rainfall are strongly influenced by the ENSO.

(*ii*) *Rainfall and winds*

The analysis of onset pentads clearly indicates that the warm phase of ENSO (CP El Niño) leads to decreased rainfall in comparison to the cold phase (La Niña) (Fig. SF1). During the onset of the ISM in La Niña (El Niño) years, the west coast of India experiences an abundance (deficit) of rainfall along with extensive (limited) spatial distribution. To improve understanding, the present analysis identifies years of late onset linked with CP El Niño and years of early onset associated with La Niña. To assess the shear-onset dynamics the wind shear composite over the CP El Niño and La Niña years separately are computed and presented in Fig. SF2. The analysis indicates that during El Niño (La Niña) years, the wind shear conditions during the monsoon onset phase typically exhibit increased (decreased) shear, which can be characterized by higher (lower) values. During El Niño years, the intensification of easterly winds at higher altitudes can result in increased wind shear in the South Indian Ocean region and the northern part of the Indian subcontinent. This phenomenon can hinder both the onset and progression of the ISM (Fig. SF2). On the other hand, during La Niña years, the opposite occurs. La Niña is characterized by weaker easterly winds at higher altitudes, which results in reduced wind shear. This reduction in wind shear is conducive to the development and progression of the ISM, often leading to an earlier and more active monsoon season with increased rainfall (SF 2b). It is evident that during El Niño years, the shear line tends to shift downward, while in La Niña years, the shear line is more prominent over the Indian subcontinent, extending in a northward direction resulting good rainfall. El Niño-related late onset years and La Niña-related early onset years are also included in the analysis to enhance comprehension. A notably pronounced positive wind shear anomaly is observed over the northern side of the Indian subcontinent and the western Indian Ocean during El Niño-associated late onset years. Conversely, during La Niña-associated early onset years, a distinct negative anomaly extends across the entire Indian region (SF4(a) and SF4(b)-upper panel).

(*iii*) *Thermodynamic aspects during CP El Niño*

To further test the linkage between convection and temperature tendency, various TDE terms are examined during CP El Nino years (SF3). During these years the diabatic heating is less prominent over KD (SF 3d) also a weaker temperature advection is visible over the Middle East and North Africa. So, from different thermodynamic terms like temperature advection and vertical motion the circulation during onset period can be well understood and the strength of the onset can be well examined.

Geopotential height and wind shear patterns during ENSO events together influence the timing and intensity of ISM onset. The analysis clearly defines that the combination of higher geopotential heights and increased wind shear during CP El Niño resulted in a delay in the onset. These atmospheric conditions make it less conducive for the establishment of the monsoon circulation and the associated rainfall. Elevated geopotential heights can also create atmospheric stability and suppress convection. This stability can delay the onset of the ISM by inhibiting the ascent of moist air parcels, which is essential for the development of monsoon rainfall. It is observed that the CP El Niño resulted in elevated geopotential heights in specific regions (Fig.SF4(a)-lower panel) along with Rossby-like circulation in wind, while conversely, La Niña years tend to exhibit the opposite pattern (Fig.SF4(b)-lower panel).

4. Conclusions

In the present study, mechanism involved in monsoon onset and its progress over the Indian subcontinent is studied emphasizing the different ENSO phases. Since, the boreal summer monsoon mean state and variability over Indian region is primarily driven by the interplay between chaotic dynamics of regional and global phenomena, this study reveals a robust connection between the thermal gradient in both zonal and meridional directions and the corresponding vertical wind shear both across the active MSD and KD domain. This relationship varies across different time scales *i.e.*, annual, seasonal (ISM-length), and onset pentad (p0), underscoring that the intensity of monsoon convection hinges on the thermal gradient and wind shear. The day-to-day variations in ISM rainfall are frequently ascribed to the chaotic nature of atmospheric dynamics. Particularly, the daily area-averaged ISM rainfall exhibits a pronounced correlation with the vertical wind shear and thermal gradient, averaged across expansive spatial areas. Analysis distinctly reveals that, during the ISM onset pentad, a positive correlation emerges between the meridional thermal gradient and wind shear over MSD and KD, leading to increased convection, with a more coherent and robust value over KD compared to MSD.

Prior to the onset of the monsoon, these wind shear conditions can disturb the convergence of moist air masses arriving from various directions, creating challenges for the establishment of the monsoon. The maximum wind height seems to be coincided with the temperature inversion height and the wind shear is observed in the low-level jet region and helps in driving the monsoon. The wind shear and thermal gradient variability also associated with the boundary layer and the convergence processes resulting convective rainfall.

Some of the key findings of the study are, 1) During the ISM onset pentad, a positive correlation emerges between the MTG and wind shear over MSD and KD, leading to increased convection. So, a strong positive correlation between MTG and wind shear is crucial for the establishment of the monsoon trough. Again, the noted correlation value is more robust in KD compared to MSD; 2) The time-height structure of daily wind, averaged over the onset pentad, reveals that there is a significant wind intensity leading to wind shears below the low-level jet core during p0 in the case of KD. Hence, domain selection proves to be crucial; 3) A weak vertical wind shear, indicates a stable state and the presence of a significant thermal gradient, characterized by minimal variations in wind speed and direction at different altitudes, are critical factors that facilitate the monsoon onset; 4) When the ITCZ shifts northward because of the thermal difference, it can alter wind shear patterns in the tropical regions. The convergence of trade winds near the ITCZ often results in weaker wind shear, creating a more favorable environment for monsoon development; 5) El Niño tends to increase wind shear over the Indian subcontinent and leads to a delayed monsoon onset. Elevated geopotential height during an El Niño year indicates the existence of a high-pressure region, which is an unfavorable condition for the onset of the monsoon; 6) The robust diabatic heating linked to monsoon generates a Gill-like Rossby wave response, initiating thermodynamic interactions with midlatitude westerly jet. This interaction results in subsidence and a subsequent reduction in rainfall along with delay in monsoon onset. The holistic understanding of these factors contributes to a comprehensive comprehension of the complex dynamics governing the onset of the ISM. This in-depth spatiotemporal examination of the linkage between various parameters and the monsoon onset serves as a valuable driver for further research into the role of large-scale atmospheric dynamics in shaping ISM onset patterns over the Indian subcontinent. Furthermore, this study also gives an indication of the influence of CP El Nino events and its influence on monsoon characteristics, which needs further exploration. Overall, this has a potential implication for operational purposes, since the ElNino and LaNina composites are exhibiting the promising results as far as the onset and its thermodynamics are concerned. The strong

predictability signal of ElNino and LaNina indicating that, the work can be used for extended range prediction and understanding the variability of monsoon onset over Indian region.

Acknowledgements

The author SL acknowledges CSIR and NCMRWF, and RD acknowledges UGC and IMD for providing the necessary facilities to carry out this research work.

Authors' Contributions

Smrutishree Lenka: Conceptualization, Data curation, Formal analysis, Investigation, Methodology, Software, Visualization, Writing – original draft, Writing – review & editing.
K.C.Gouda: Conceptualization, Funding acquisition, Investigation, Supervision, Writing – review & editing.
Mohan. T. S: Formal analysis, Investigation, Supervision, Writing – review & editing.
Rani Devi: Data curation, Formal analysis, Investigation, Software, Validation, Writing – review & editing.

Disclaimer

Authors confirm that this work is original and has not been published elsewhere, nor is it currently under consideration for publication elsewhere.

References

Abu-Hamdeh, N. H., 2003, "Thermal properties of soils as affected by density and water content", *Biosystems engineering*, **86**, 1, 97-102.

Ananthakrishnan, R., & Soman, M. K., 1988, "The onset of the southwest monsoon over Kerala: 1901–1980", *J. Climatol*, ***8***, 3, 283-296.

Ashok, K., Guan, Z., & Yamagata, T. (2003). A look at the relationship between the ENSO and the Indian Ocean dipole. *Journal of the Meteorological Society of Japan. Ser. II*, **81**, 1, 41-56.

Ashok, K., Guan, Z., Saji, N. H., & Yamagata, T., 2004, "Individual and combined influences of ENSO and the Indian Ocean dipole on the Indian summer monsoon", *Journal of Climate*, **17**, 16, 3141-3155.

Athira, U. N., Abhilash, S., & Sabeerali, C. T., 2023, "Paradigm shift in the onset phase of the Indian Summer Monsoon since 2000 and its potential connection to South Indian Ocean", *Atmospheric Research*, **296**, 107050.

Belmecheri, S., Babst, F., Hudson, A. R., Betancourt, J., & Trouet, V. 2017, "Northern Hemisphere jet stream position indices as diagnostic tools for climate and ecosystem dynamics", *Earth Interactions*, **21**, 8, 1-23.

Devi, R., Gouda, K. C., & Lenka, S., 2024, "Assessment of long-term spatio-temporal variability of hot extremes and associated physical mechanism over India", *Stochastic Environmental Research and Risk Assessment*, **38**, 8, 3257-3272.

Douglas, M. W., 1992, "Structure and dynamics of two monsoon depressions", Part I: Observed structure. *Monthly weather review*, **120**, 8, 1524-1547.

Duan, A., Sui, C., & Wu, G., 2008, "Simulation of local air-sea interaction in the great warm pool and its influence on Asian monsoon", *Journal of Geophysical Research: Atmospheres*, **113**, D22.

ENSO and the Indian Ocean dipole on the Indian summer monsoon. *Journal of Climate*, **17**, 16, 3141-3155.

Fasullo, J., & Webster, P. J. (2003). A hydrological definition of Indian monsoon onset and withdrawal. *Journal of Climate*, **16**, 19, 3200-3211.

Gadgil, S., 2018, The monsoon system: Land–sea breeze or the ITCZ? *Journal of Earth System Science*, **127**, 1-29.

Gadgil, Sulochana. "The Indian monsoon and its variability." *Annual Review of Earth and Planetary Sciences* 31.1 (2003): 429-467.

Geen, R., Bordoni, S., Battisti, D. S., and Hui, K., 2020, "Monsoons, ITCZs, and the concept of the global monsoon", *Reviews of Geophysics*, **58**, 4, e2020RG000700.

Goswami, B. N., Krishnamurthy, V., & Annmalai, H., 1999, "A broad-scale circulation index for the interannual variability of the Indian summer monsoon", *Quarterly Journal of the Royal Meteorological Society*, **125**, 554, 611-633.

Gouda, K. C., & Goswami, P., 2016, "Organization of vertical shear of wind and daily variability of monsoon rainfall", *Meteorology and Atmospheric Physics*, **128**, 5, 565-577.

Hastenrath, S., & Greischar, L., 1991, "The monsoonal current regimes of the tropical Indian Ocean: Observed surface flow fields and their geostrophic and wind-driven components", *Journal of Geophysical Research: Oceans*, **96**, C7, 12619-12633.

Hersbach, H., Bell, B., Berrisford, P., Hirahara, S., Horányi, A., Muñoz-Sabater, J., ... & Thépaut, J. N., 2020, "The ERA5 global reanalysis", *Quarterly journal of the royal meteorological society*, **146**, 730, 1999-2049.

Hoskins, B. J., & Karoly, D. J., 1981, "The steady linear response of a spherical atmosphere to thermal and orographic forcin",. *Journal of Atmospheric Sciences*, **38**, 6, 1179-1196.

Hoskins, B. J., & Rodwell, M. J. (1995). A model of the Asian summer monsoon. Part I: The global scale. *Journal of Atmospheric Sciences*, **52**, 9, 1329-1340.

Jain, Sharad K., and Vijay Kumar. "Trend analysis of rainfall and temperature data for India." *Current science* (2012): 37-49.

Kripalani, R. H., Kulkarni, A., Sabade, S. S., & Khandekar, M. L., 2003, "Indian monsoon variability in a global warming scenario", *Natural hazards*, **29**, 189-206.

Lenka, S., Devi, R., Joseph, C. M., & Gouda, K. C., 2022, "Effect of large-scale oceanic and atmospheric processes on the Indian summer monsoon", *Theoretical and Applied Climatology*, **147**, 3, 1561-1576.

Lenka, S., Gouda, K. C., Devi, R., and Joseph, C. M., 2024, "Dynamics of Indian summer monsoon in different phases", *Climate Dynamics*, **62**, 1, 473-495.

Li, C., & Yanai, M., 1996, "The onset and interannual variability of the Asian summer monsoon in relation to land–sea thermal contrast", *Journal of Climate*, **9**, 2, 358-375.

Mohanty, U. C., Ramesh, K. J., Kumar, N. M., and Potty, K. V. J., 1994, "Variability of the Indian summer monsoon in relation to oceanic heat budget over the Indian seas", *Dynamics of atmospheres and oceans*, **21**, 1, 1-22.

Moron, Vincent, and Andrew W. Robertson. "Interannual variability of Indian summer monsoon rainfall onset date at local scale." *International journal of climatology* 34.4 (2014).

Pai, D. S., Rajeevan, M., Sreejith, O. P., Mukhopadhyay, B., & Satbha, N. S., 2014, "Development of a new high spatial resolution (0.25× 0.25) long period (1901-2010) daily gridded rainfall data set over India and its comparison with existing data sets over the region. *Mausam*, **65**, 1, 1-18.

Parthasarathy, B., & Yang, S., 1995, "Relationships between regional Indian summer monsoon rainfall and Eurasian snow cove", *Advances in atmospheric sciences*, **12**, 143-150.

Prasad, V. S., & Hayashi, T., 2005, "Onset and withdrawal of Indian summer monsoon", *Geophysical research letters*, **32**, 20.

Privé, N. C., & Plumb, R. A., 2007, "Monsoon dynamics with interactive forcing. Part I: Axisymmetric studies. *Journal of the atmospheric sciences*, **64**, 5, 1417-1430.

Rao Y P 1976 Southwest monsoon India Meteorological Department; *Meteorological Monograph Synoptic Meteorology*, **No. 1/1976**, Delhi, 367 pp.

Roy, I., Tedeschi, R., & Collins, M., 2016, ENSO teleconnections to the Indian summer monsoon in observations and models.

Sahana, A. S., Ghosh, S., Ganguly, A., & Murtugudde, R., 2015, "Shift in Indian summer monsoon onset during 1976/1977", *Environmental Research Letters*, **10**, 5, 054006.

Soman, M. K., & Kumar, K. K., 1993, "Space-time evolution of meteorological features associated with the onset of Indian summer monsoon", *Monthly Weather Review*, **121**, 4, 1177-1194.

Wang, B., & Ding, Q., 2008, "Global monsoon: Dominant mode of annual variation in the tropics", *Dynamics of Atmospheres and Oceans*, **44**, 3-4, 165-183.

Wang, B., Ding, Q., & Joseph, P. V., 2009, "Objective definition of the Indian summer monsoon onset", *Journal of Climate*, **22**, 12, 3303-3316.

Webster, P.J. and Yang, S., 1992, "Monsoon and ENSO: Selectively Interactive Systems. Quarterly Journal of the Royal Meteorological Society, 118, 877-926. U http://dx.doi.org /10.1002/qj.49711850705U

Webster, Peter J., et al.1998, "Monsoons: Processes, predictability, and the prospects for prediction." *Journal of Geophysical Research: Oceans* **103**.C7 : 14451-14510.

Weldeab, S., Rühlemann, C., Ding, Q., Khon, V., Schneider, B., & Gray, W. R. (2022). Impact of Indian Ocean surface temperature gradient reversals on the Indian Summer Monsoon. *Earth and Planetary Science Letters*, **578**, 117327.

Wilson, S. S., & Mohanakumar, K., 2020, "A new circulation index for the detection of monsoon intensity", *International Journal of Climatology*, **40**, 3, 1900-1908.

Yamada, T. J., Shrivastava, S., & Kato, R., 2022, "Land–sea thermal contrast associated with summer monsoon onset over the Chao Phraya River basin", *Theoretical and Applied Climatology*, **150**, 1, 73-83.

Yanai, M., & Tomita, T., 1998, "Seasonal and interannual variability of atmospheric heat sources and moisture sinks as determined from NCEP–NCAR reanalysis. *Journal of Climate*, **11**, 3, 463-482.

Yanai, M., Esbensen, S., & Chu, J. H. (1973). Determination of bulk properties of tropical cloud clusters from large-scale heat and moisture budgets. *Journal of Atmospheric Sciences*, **30**, 4, 611-627.

Appendix

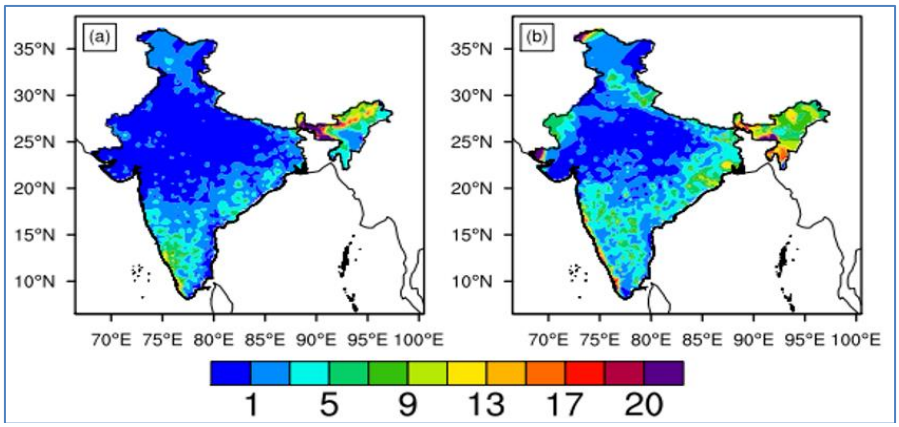

Fig. SF 1. Spatial distribution of (a) CP Elnino and (b) Lanina rainfall averaged over the onsetntad

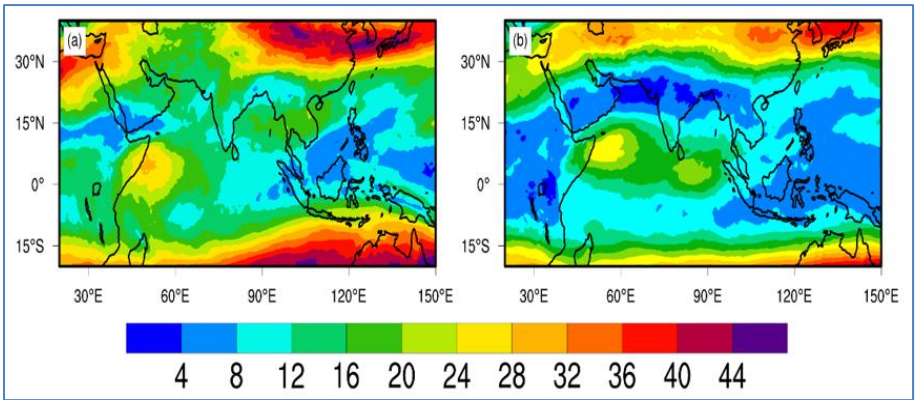

Fig. SF 2. Spatial distribution of wind shear climatology at (a) CP Elnino (850 hPa) and (b) Lanina (850hPa), averaged over the onset pentad duration

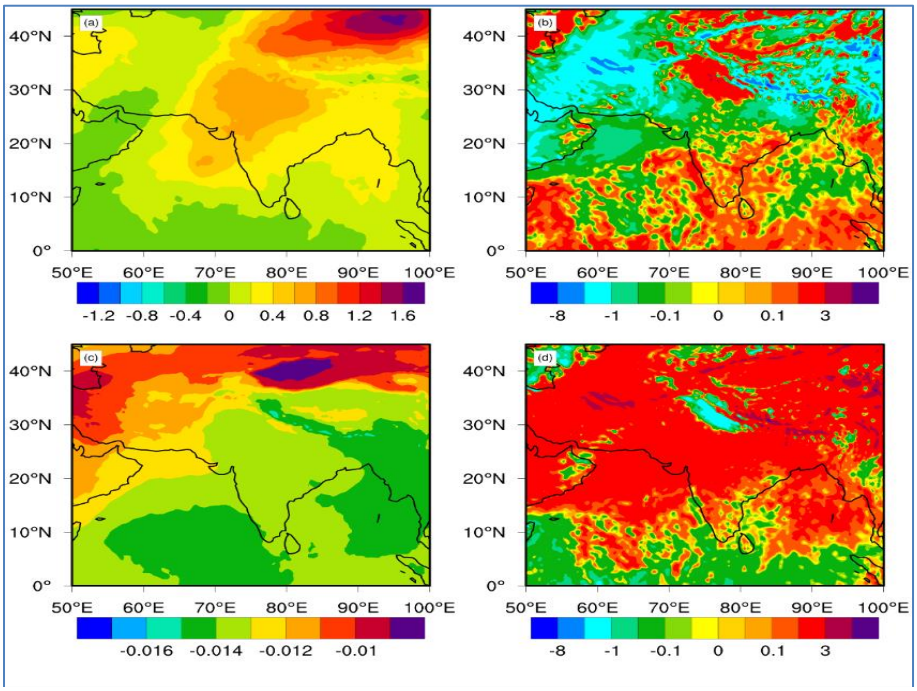

Fig. SF3. Illustration of the four individual terms of the dry thermodynamic equation at 700 – 250 hPa for CP ElNino year, namely (a) temperature advection (b) horizontal advection (c) static stability and (d) diabatic heating

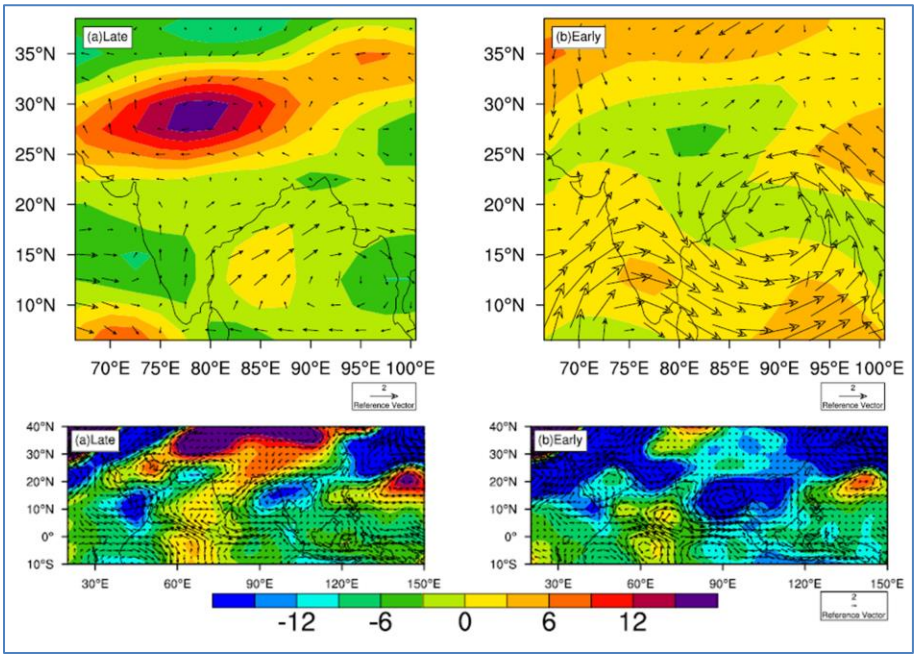

Fig. SF4. Spatial maps of anomalous wind shear: Upper Panel - (a) CP El Nino related late onset composite map and (b) La Nina associated early onset composite; 500 hPa geopotential height anomalies and wind vectors: Lower panel - (a) CP El Nino related late onset and (b) La Nina associated early onset composite map